

ANTIMONY-DOPED TIN OXIDE NANOSTRUCTURES PREPARED BY SOL-GEL DIP COATING METHOD

Sabar D. Hutagalung, Khatijah A. Yaacob and Lee B. Yeow

*School of Materials and Mineral Resources Engineering, Universiti Sains Malaysia,
14300 Nibong Tebal, Penang, Malaysia*

ABSTRACT

Tin oxide (SnO_2) thin films are widely used as a gas sensor that can change their resistance during interaction with molecular gases. One of the most important factors that influence the sensitivities of sensing material is its structural properties especially surface morphology. In this work, we present preparation and characterization of undoped and antimony-doped tin oxide ($\text{Sb}:\text{SnO}_2$) thin film nanostructures for gas sensing applications. The SnO_2 thin films were deposited by sol-gel dip coating method onto glass substrates and sintered at $500\text{ }^\circ\text{C}$ in air. Sb dopant concentration was varied from 1 to 4 mol% to investigate the effect of doping on the electrical and sensing properties. The films were characterized by XRD, SEM and AFM. The SEM and AFM images of films showed a very smooth surface morphology with nanostructure grain size in the range of 37.6 to 56.3 nm. Sensing sensitivity of $\text{Sb}:\text{SnO}_2$ films are much higher than undoped films.

INTRODUCTION

Transparent conducting oxide, such as tin oxide (SnO_2) thin films have been widely investigated due to their large range of applications in photovoltaic cells, liquid crystal display, photodetectors, gas sensors, etc. [1–9]. SnO_2 also has been proposed as a promising alternative anode material for microbatteries. It has been reported that its theoretical volumetric capacity is four times larger than that of carbon-based material, while its gravimetric capacity is twice as large [10]. Undoped or doped SnO_2 thin films have been prepared by using several methods such as sol-gel [2,9,11], mechanomechanical [5,12], liquid flow deposition [6], and spray pyrolysis [13]. Sol-gel coatings generally consist of thin films deposited on solid substrates from a liquid solution. The films are generally deposited by dip coating, but may also be deposited using spin coating or other thin film deposition techniques [11]. Dip coating techniques can be described as a process where the substrate to be coated is immersed in a liquid and then withdrawn with a well-defined withdrawal speed under controlled temperature and atmospheric conditions. The coating thickness is mainly defined by the withdrawal speed, solid content and viscosity of the liquid. To achieve uniform defect-free deposition, the substrate must be free of dust and other particles and it must be uniformly wetting to the sol-gel solution used to deposit the film.

The interesting part of dip coating processes is that by choosing an appropriate viscosity the coating thickness can be varied with high precision and quality. The atmosphere controls the evaporation of the solvent and the subsequent destabilization of

the sols by solvent evaporation, leads to a gelatine process and the formation of a transparent film due to the small particle size in the sols (nm range) [14]. One of the main problems using tin and antimony alkoxides in sol-gel process is their high sensitivity to moisture and difficult to control the thickness of the films versus viscosity [15]. In this work, undoped and Sb-doped SnO₂ thin film nanostructures were prepared by sol-gel dip coating technique using the colloidal precursors of SnCl₄ and SbCl₃ aqueous solution.

EXPERIMENTAL DETAILS

Tin(IV) chloride pentahydrate (SnCl₄.5H₂O), antimony chloride (SbCl₃), urea (NH₂CONH₂), and hydrochloric acid (HCl) were used to prepare the precursor solution. Aqueous precursors of SnCl₄ (0.2 M), HCl (1 M), urea (4 M) and various amount of SbCl₃ (0 – 4 mol%) were prepared in a three-neck flash. The initial pH of the precursor solution is 1 and the final pH value was controlled to be 8. Suspended white sol (undoped) or brown sol (Sb-doped) was obtained by refluxing the precursor at 100 °C for 2 hours. SnO₂ thin films were deposited on pre-cleaned glass substrates by dip coating technique at room temperature. The substrates were dipped vertically, left for 20 sec, and withdrawn from the sol at a constant rate of 5 mm/min. After dipping, the films were dried at 100 °C for 30 min in air and followed by heating at 300 °C for 1 hour. To further increase the thickness, the sequence of dipping, drying, heating and then dipping again was performed a number of times. The sintering at 500 °C for 1 hour was however done only after the final dipping process.

Film thickness was measured by Filmetrics F20. The surface morphology and microstructure were investigated by scanning electron microscopy (SEM) and atomic force microscope (AFM), which is also used to determine the surface roughness. The crystallinity of the films was examined by X-ray diffraction (XRD) with CuK α radiation. Interdigitated Au/Pd electrodes were deposited onto the surface of films for sensing application. The gas-sensing activity was tested at room temperature where sensor element was put in the glass tube and CO₂ gas injected into the tube with constant flow rate. The resistance was continuously monitored during gas running out.

RESULTS AND DISCUSSION

The thickness of the undoped and Sb-doped SnO₂ thin films were found to increase almost linearly with respect to the number of dipping (in the range of 148.0 to 155.5 nm for 1 to 5 dipping number).

XRD pattern taken from the sample of 4 mol% Sb:SnO₂ thin films (Figure 1) confirmed the crystallographic phases present in the film with five-strongest diffraction peaks belonging to SnO₂ and Sb₂O₄. The rest of the samples with antimony doping concentration of 3 mol% or less (XRD results not shown) were found that there were no additional peaks to SnO₂. Meanwhile, the rest of the films were pure SnO₂ phase and Sb dopant did not form a second phase either in or with the tin oxide. As the amount of Sb dopant increases to 4 mol%, the XRD result shows the existence of Sb₂O₄ in SnO₂ matrix (Figure 1). It could be due to oxidation of orthorhombic valentinite (Sb₂O₃)

transforming to orthorhombic cervantite (Sb_2O_4) phase by diffusion of oxygen atom process [16].

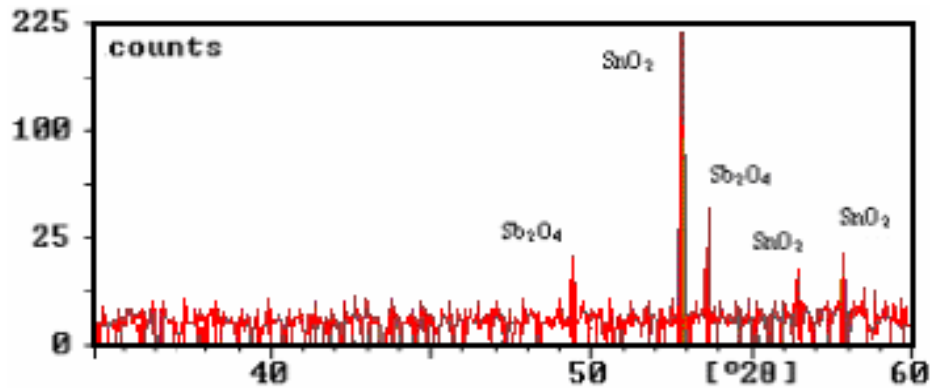


Figure 1: XRD result of 4 mol% Sb:SnO₂ thin films.

SEM micrograph shows that surface of undoped SnO₂ thin films are smoother than Sb-doped films (Figure 2). The films consist of small particles distributed on the surface that shows nanostructure properties. The more amounts of Sb was deteriorates the smoothness of the films surface, and at the surface of films doped with 4 mol% Sb was observed existence of some big particles. This phenomenon may be due to grow up of grains of dopant material and form antimony oxide phase in solid solution with tin oxide.

The surface morphology of the undoped SnO₂ thin films as revealed by the AFM image is shown in Figure 3 on a scanning area of 500 nm x 500 nm. The average roughness, R_a of sample is in the order of 0.78 nm, whereas the peak-to-valley roughness, R_{PV} takes value of up to 5.19 nm (Figure 3c). This result indicates that the coating surface morphology of SnO₂ thin films is almost perfectly smooth with nanosize grains. The estimated grain size of undoped films is in the range of 37.6 – 56.3 nm. Figure 4 shows the AFM images on a scanning area of 2 μm x 2 μm of Sb-doped SnO₂ thin films with dopant concentration in the range of 1 to 4 mol%. It was observed that the undoped SnO₂ thin films surface was smooth (Figure 3a), whereas the Sb-doped SnO₂ thin films showed a relatively rough and porous surface (Figure 4). The average roughness and peak-to-valley roughness of Sb:SnO₂ thin films are in the range of 4.26 to 23.37 nm and 32.13 to 91.36 nm, respectively.

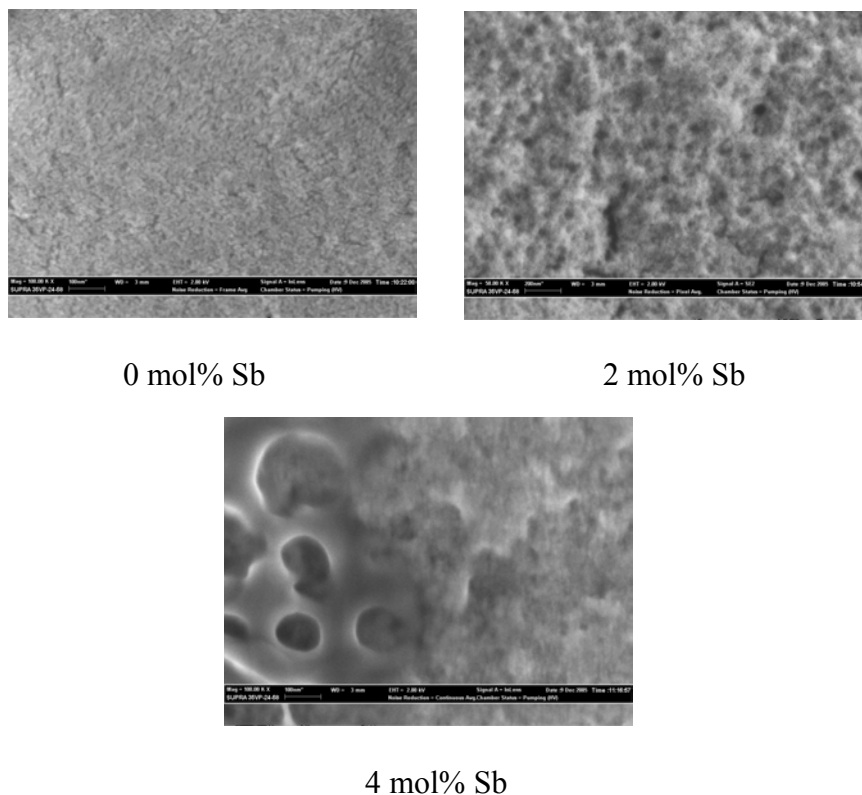


Figure 2: SEM micrographs of undoped and Sb-doped SnO₂ thin films.

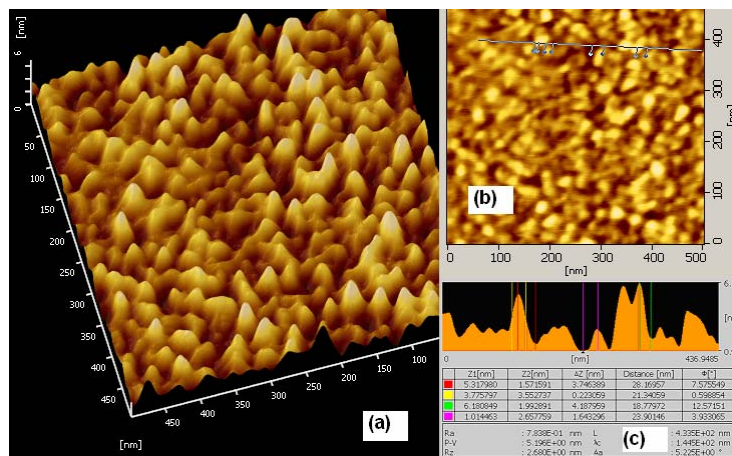


Figure 3: AFM images of undoped SnO₂ thin films: (a) 3D image, (b) 2D image, (c) height profile along the line indicated in (b).

Figure 5 shows the effect of Sb-dopant concentration on the sheet resistance and sensitivity of SnO₂ thin films. The sheet resistance of pure and Sb-doped films was found to decrease with increasing dopant concentrations. Gas response of undoped and Sb-doped SnO₂ thin films were measured in the flowing of CO₂ gas with constant flow

rate of 200 ml/min and measured at room temperature. The sensitivity, S of films was defined by:

$$S = \frac{(R_o - R_g)}{R_o} \quad (1)$$

where R_o is the resistance of films in air, and R_g the resistance in gas [6]. The response curve shows that the sensitivity of undoped SnO_2 thin films is much lower than Sb-doped films, which is less than 10% for undoped films, whereas sensitivity of Sb-doped films more than 30%. However, the doping concentration did not affect very much the sensitivities of Sb: SnO_2 thin films.

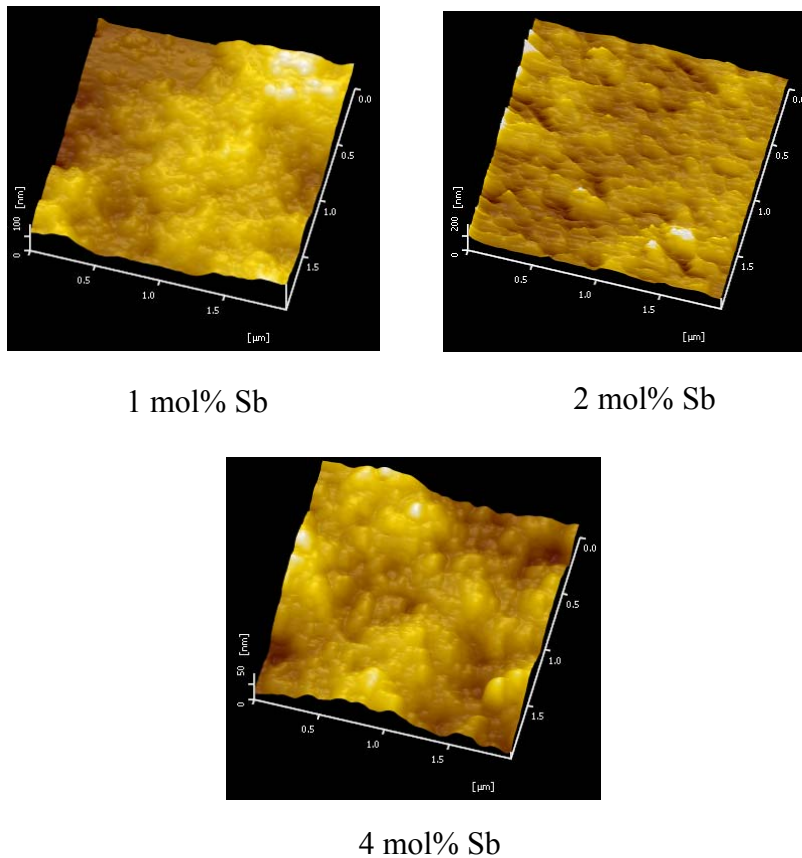


Figure 4: The 3D AFM images of Sb-doped SnO_2 thin films.

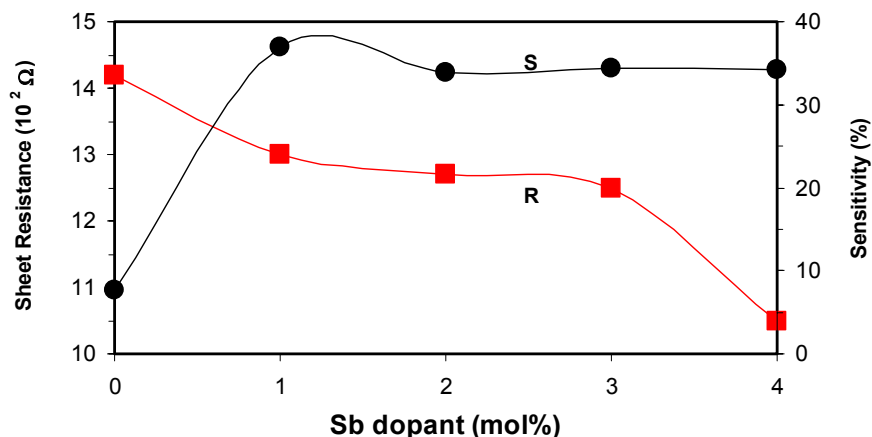
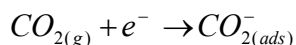


Figure 5: Effect of doping concentration on the sheet resistance in air and sensitivity of SnO₂ thin films in CO₂ gas.

Sheet resistance of thin films when exposed to CO₂ gas was found lower than in air. This result can be explained as CO₂ surface chemisorptions and gain electron depletion. In fact CO₂ molecules can be directly adsorbed and interact with the oxygen adsorbed onto the sensor surface. The involved reactions are:



(2)



The adsorbed ions CO₂⁻ are desorbed, with a rate dependent on the temperature, as CO₂ gas, recovering the initial conditions. The obtained resistivities were in a good agreement with those reported by Terry et al. [11] and Hu and Hou [15], whereas the sensitivity was lower than report by Chatterjee et al. [17].

CONCLUSION

Undoped and Sb-doped SnO₂ thin films have been obtained by sol-gel multidipped coating method using the colloidal precursors from Sn and Sb chloride aqueous solutions. The prepared SnO₂ films were shown a nanosize structure with a relatively smooth surface morphology. Sensing properties toward CO₂ gas was found that sensitivity of Sb:SnO₂ films are higher than undoped SnO₂ films.

ACKNOWLEDGEMENT

This work was supported by USM Short Term Grant No. 304/PBahan/6035119 and IRPA Project No. 09-02-05-4086-SR0013. The authors also wish to thank Ms. Kio Nakamura, SII Nanotechnology, Japan for technical assistance on AFM analysis.

REFERENCES

- [1] Onyia, A. I, Okeke, C. E. (1989); *J. Phys. D: Appl. Phys.* **22**, 1515.
- [2] Rella, R., Serra, A., Siciliano, P., Vasanelli, R., De, G., Licciulli, A., Quirini, A. (1997); *Sensor & Actuators B* **44**, 462.
- [3] Siciliano, P. (2000); *Sensor & Actuators B* **70**, 153.
- [4] Emiroglu, S., Barsan, N., Weimar, U., Hoffmann, V. (2001); *Thin Solid Films* **391**, 176.
- [5] Cukrov, L. M., McCormick, P. G., Galatsis, K., Wlodarski, W. (2001); *Sensor & Actuators B* **77**, 491.
- [6] Supothina, S. (2003); *Sensor & Actuators B* **93**, 526.
- [7] Hyodo, T., Abe S., Shimizu Y., Egashira M. (2003); *Sensor & Actuators B* **93**, 590.
- [8] Niranjana, R. S., Hwang, Y. K., Kim, D.-K, Jhung, S. H., Chang, J. -S, Mulla, I. S. (2005); *Mater. Chem. Phys.* **92**, 384.
- [9] Guzman, G., Dahmani, B., Puetz, J., Aegerter, M. A. (2006); *Thin Solid Films* **502**, 281.
- [10] Huang, H., Kelder, E. M., Chen, L. (1999); *J. Power Sources* **81-82**, 362.
- [11] Terrier, C., Chatelon, J. P., Roger, J. A. (1997); *Thin Solid Films* **295**, 95.
- [12] Galatsis, K., Cukrov, L., Wlodarski, W., McCormick, P. (2003); *Sensor & Actuators B* **93**, 562.
- [13] Elengovan, E., Shivashankar, S. A., Ramamurthi, K. (2005); *J. Crys. Growth* **276**, 215.
- [14] Brinker, C. J., Hurd, A. J., Ward, K. J. (1988); *Ultrastructure Processing of Advanced Ceramics*, eds. J. D. Mackenzie and D. R. Ulrich, Wiley, pp. 223.
- [15] Hu, Y. and Hou, S. -H. (2004); *Mater. Chem. Phys.* **86**, 21.
- [16] Gopalakrishnan, P. S., and Manphar, H. (1976); *J. Sol. State Chem.* **16**, 301.
- [17] Chatterjee, K., Chatterjee, S., Banerjee, A., Raut, M., Pal, N. C., Sen, A., and Maiti, H. S. (2003); *Mater. Chem. Phys.* **81**, 33.